https://ntrs.nasa.gov/search.jsp?R=20180000086 2018-07-26T05:27:55+00:00Z

Heavy Ion Testing at the Galactic Cosmic Ray Energy Peak

Jonathan A. Pellish, Michael A. Xapsos, Kenneth A. LaBel, Paul W. Marshall, David F. Heidel, Kenneth P. Rodbell, Mark C. Hakey, Paul E. Dodd, Marty R. Shaneyfelt, James R. Schwank, Robert C. Baumann, Xiaowei Deng, Andrew Marshall, Brian D. Sierawski, Jeffrey D. Black, Robert A. Reed, Ronald D. Schrimpf, Hak S. Kim, Melanie D. Berg, Michael J. Campola, Mark R. Friendlich, Christopher E. Perez, Anthony M. Phan, and Christina M. Seidleck

***Abstract*—A 1 GeV/u ^{56}Fe ion beam allows for true 90° tilt irradiations of various microelectronic components and reveals relevant upset trends at the GCR flux energy peak. Three SRAMs and an SRAM-based FPGA evaluated at the NASA Space Radiation Effects Laboratory demonstrate that a 90° tilt irradiation yields a unique device response. These tilt angle effects need to be screened for, and if found, pursued with radiation transport simulations to quantify their impact on event rate calculations.**

I. Introduction

ACCELERATED ground testing using heavy ions to study single-event effects (SEE) in microelectronic components differs from the actual space environment in two critical ways: one, ground-based accelerator heavy ion fluxes are much larger and two, ground-based accelerators cannot produce ions that cover the high-energy regime in space [1]. While these two issues do not prevent effective ground-based characterization of SEE, they tend to limit experimental conditions, some of which are important for hardness assurance. This paper describes recent heavy ion single-event upset (SEU) experiments at the NASA Space Radiation Effects Laboratory at Brookhaven National Laboratory using a ^{56}Fe beam with energies of 0.1, 0.5, and 1 GeV/u. These energies correspond to silicon linear energy transfers (LET) of 3.9, 1.5, and 1.2 (MeV · cm^2)/mg. The devices under consideration include static random access memories (SRAM) and a SRAM-based field programmable gate array (FPGA).

Manuscript received 11 September 2009. This work was supported in part by the NASA Electronic Parts and Packaging program, the Space Radiation Element Human Research program at NASA/JSC, and the Defense Threat Reduction Agency Radiation Hardened Microelectronics Program under *IACRO* #09-4587I to NASA and #09-4584I to SNL. Sandia is a multiprogram laboratory operated by Sandia Corporation, a Lockheed Martin Company, for the United States Department of Energy's National Nuclear Security Administration under Contract DE-AC04-94AL85000.

J. A. Pellish, M. A. Xapsos, and K. A. LaBel are with the Radiation Effects and Analysis Group, NASA/GSFC Code 561.4, 8800 Greenbelt RD, Greenbelt, MD 20771 USA. (email: jonathan.a.pellish@nasa.gov)

P. W. Marshall is a NASA consultant, Brookneal, VA 24528 USA.

D. F. Heidel and K. P. Rodbell are with the IBM T. J. Watson Research Center, Yorktown Heights, NY 10598 USA.

M. C. Hakey is with the IBM System and Technology Group, Essex Junction, VT 05452 USA.

P. E. Dodd, M. R. Shaneyfelt, and J. R. Schwank are with Sandia National Laboratories, Albuquerque, NM 87185 USA.

R. C. Baumann, X. Deng, and A. Marshall are with Texas Instruments, Dallas, TX 75243 USA.

B. D. Sierawski, J. D. Black, R. A. Reed, and R. D. Schrimpf are with the Department of Electrical Engineering and Computer Science, Vanderbilt University, Nashville, TN 37235 USA.

H. S. Kim, M. D. Berg, M. J. Campola, M. R. Friendlich, C. E. Perez, A. M. Phan, and C. M. Seidleck are with MEI Technologies (NASA/GSFC), Greenbelt, MD 20771 USA.

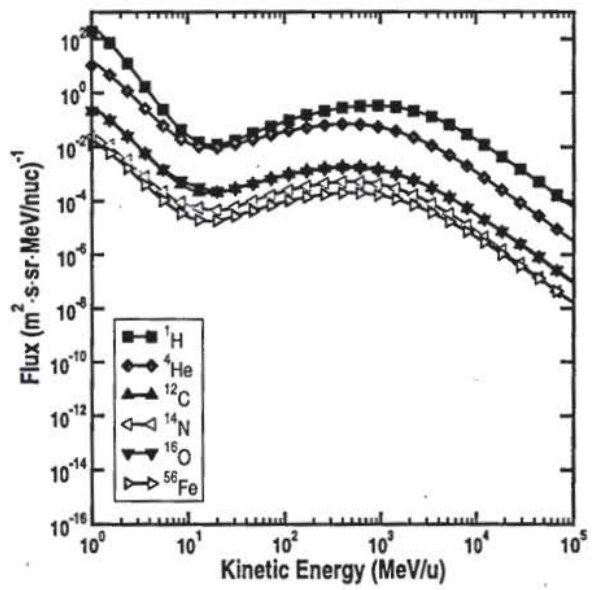

Fig. 1. Heavy ion fluxes for all the naturally occurring elements in space. The levels are representative of a geostationary orbit at solar minimum; anisotropy is not included. Note that the flux-energy peak occurs at a kinetic energy of approximately 1 GeV/u. The grayed-out traces below ^{56}Fe are the rest of the elements not represented in the legend. GCR abundance is, in general, inversely proportional to the atomic number, Z.

Spacecraft must be designed to handle a number of different radiation environment hazards, including, but not limited to particle radiation, electromagnetic radiation, and orbital debris [2]. This work considers SEU hardness assurance for microelectronic components and thus focuses on the three categories of high-energy particle radiation in space. There are particles trapped in planetary magnetic fields, high fluxes of protons and heavy ions emitted from the sun during coronal mass ejections and solar flares, and a low flux, isotropic background of protons and heavy ions originating outside of the solar system called galactic cosmic rays (GCR), like those shown in Fig. 1. It is the third category, GCR, that is relevant here.

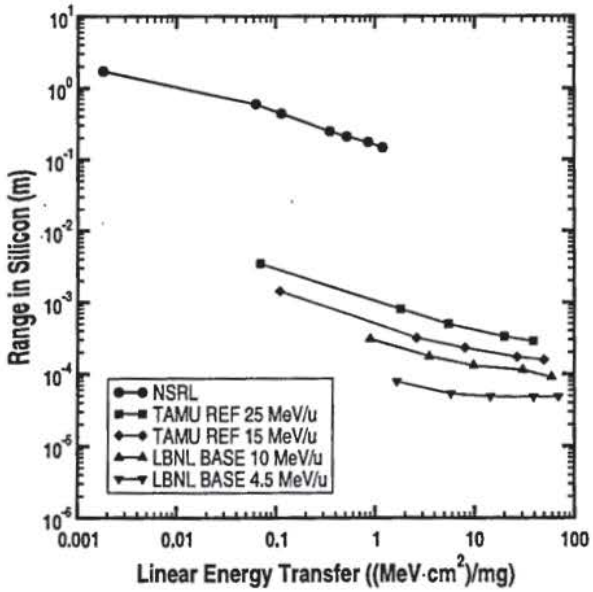

Fig. 2. The range *vs.* LET_{Si} characterizations of two representative heavy ion facilities relative to the NSRL. Note that the JYFL RADEF facility's K-130 cyclotron produces beams similar to LBNL BASE 10 and 4.5 MeV/u [8]. Ranges and LET values shown are for silicon. Note that the NSRL beams, at 1 GeV/u, are representative of the flux energy peak of the GCR spectrum. The NSRL data points represent hydrogen, carbon, oxygen, silicon, chlorine, titanium, and iron. The Texas A&M University (TAMU) REF data points come from helium, neon, argon, krypton, and xenon. The Lawrence Berkeley National Laboratory (LBNL) BASE data points come from boron, neon, argon, krypton, and xenon. All values are calculated at normal incidence.

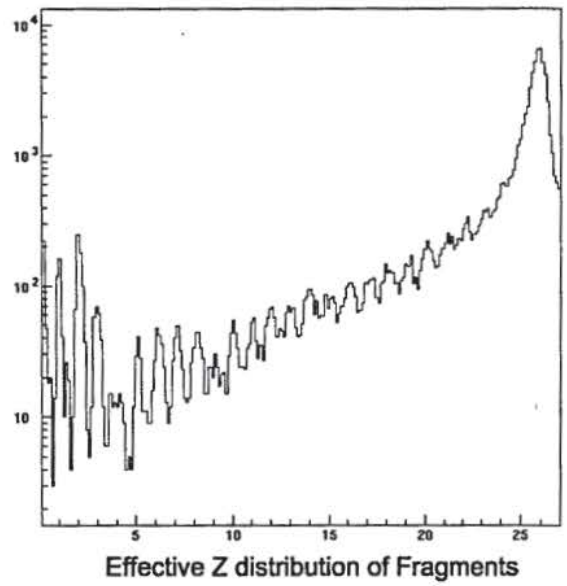

Fig. 3. The effective-Z distribution of the fragments detected in a scintillator placed in a narrow (1 cm diameter) beam of 1 GeV/u ^{56}Fe with an air target at the NSRL. The well-known suppressions are seen at $Z = 4$ and $Z = 9$. The image is courtesy of M. Siverts [23].

GCR include all naturally occurring elements and have a flux energy peak of approximately 1 GeV/u [2]–[7], as shown in Fig. 1. GCR abundance is inversely proportional to the atomic number, Z, with the exception of iron, which accounts for a large amount of the total GCR flux beyond oxygen. These high-energy cosmic rays are very penetrating and have low LET values. While the GCR spectrum has higher LET components, they have a much lower flux. Nevertheless, accelerated ground testing includes higher LET values to thoroughly characterize component response.

$$\Omega = 2\pi\left[1 - \cos\left(\frac{a}{2}\right)\right] \qquad (1)$$

The maximum angle of irradiation in typical ground-based accelerator testing is governed by the device under test's (DUT) packaging and the range of the ion. While accelerated testing is often conducted at tilt angles between normal incidence and a maximum of perhaps 60-70°, half of the GCR flux is incident at angles greater than 60°. The solid angle of a cone, shown in Eq. 1, can be used to approximate a plane of sensitive devices. When the apex, a, is equal to 120°, $\Omega = \pi$, which is half the solid angle subtended by the surface of a hemisphere [9]. This means that half of the particles in an isotropic environment are incident at angles below 60° and the other half at angles above 60°.

Since a large number of heavy ions in the GCR spectrum are incident at grazing angles relative to the surface normal of the part, multiple-bit/cell upset (MBU) will be a significant concern [10]–[12]. MBUs are problematic because they can reduce or negate the effectiveness of error detection and correction codes [13]. This hardness assurance concern is further complicated by the fact that modern, highly-scaled process technologies ($\leq$ 100 nm) are more sensitive to MBU [14]–[18]. This is the result of packing the sensitive nodes closer together and not necessarily an increase in upset sensitivity, particularly for technologies below 90 nm [19]. In several cases, the upset thresholds of these technologies are low enough to be affected by direct ionization from incident protons [19]–[22].

II. Experimental Facility and Setup

The NASA Space Radiation Laboratory (NSRL) at Brookhaven National Laboratory (BNL) is a joint effort by the NASA Johnson Space Flight Center and the Department of Energy's Office of Science designed to study radiobiological effects relevant to human spaceflight. In addition to radiobiological studies, the NSRL also hosts physics experiments such as this work. Currently, heavy ions are accelerated using one of the two BNL Tandem van de Graaff accelerators and sent down a 700 m beamline to the Booster synchrotron. The beams are accelerated further in the Booster and then delivered to the NSRL. Because the Tandems serve as the ion source, the number of beams available at the NSRL is presently limited to hydrogen, carbon, oxygen, silicon, chlorine, titanium, and iron. However, with the commissioning of the electron beam ion source in 2010, all ions from hydrogen to uranium will be available and at much higher fluxes.

The NSRL 1 GeV/u particle beams are compared to two other common facilities' beam selections in Fig. 2. The NSRL beams favor low LETs and substantial ranges, just like the

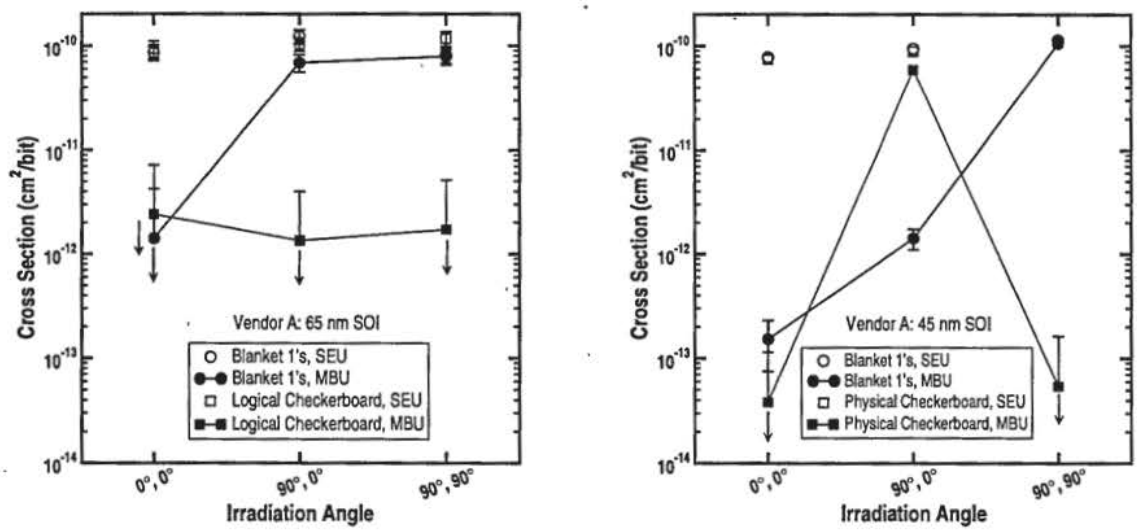

(a) Vendor A's 65 nm, 1 Mbit SOI SRAM

(b) Vendor A's 45 nm, 36 Mbit SOI SRAM

Fig. 4. Vendor A's ^{56}Fe data. The abscissa categories are given as (ϕ, θ) tilt/roll angle pairs. The legend shows the data pattern and the type of upset cross section. All irradiations used the 1 GeV/u ^{56}Fe beam. The 65 nm SOI SRAM in Fig. 4(a) was biased with $V_{DD} = 1.3$ V and the 45 nm SOI SRAM in Fig. 4(b) was biased with $V_{DD} = 1.3$ V. Limiting cross sections are indicated by downward-pointing arrows.

actual space environment. With the recent addition of low-LET beams at both Texas A&M University and Lawrence Berkeley National Laboratory, there is some LET commonality between the NSRL and these other two facilities. However, the substantial energy increase at the NSRL translates to a 30x difference in range for overlapping LETs. It is becoming necessary to use these lower LET beams when searching for SEE onset due to increasing technology sensitivity [19] and the corresponding impact on SEE rate calculations.

The NSRL operators spent considerable time and effort characterizing the iron beam, including fragmentation behavior. Knowledge of the heavy ion fragmentation cross sections are necessary in order to deliver a clean beam, dominated by the accelerated primary species, ^{56}Fe in this case. Fig. 3 shows a fragmentation spectrum for the 1 GeV/u ^{56}Fe beam using both scintillators and silicon detectors. The spectrum is dominated by iron at $Z = 26$, with the well-known suppressions at $Z = 9$ and $Z = 4$. A similar spectrum was measured by Y. M. Charara using a thin silicon detector in the process of validating the radiation transport code HETC-HEDS [24].

The beam itself is well-controlled and focused by two sets of magnetic lenses that can produce a "square" beam spot of up to 20 cm × 20 cm with a uniformity of ±2%; this was the beam used in this work. The staple energy tune at the NSRL is 1 GeV/u, though the energy can be changed quickly if the facility is given adequate notice of the required tunes. The energy range is approximately 0.1 GeV/u to 1 GeV/u, which is the energy at the DUT, not the extraction energy of the Booster synchrotron. At lower energies the beam is less uniform, with a small dip in intensity at the center of the beam spot. The ions are delivered to the target room in 300 ms spills approximately every 3.7 s. Real-time dosimetry is achieved with a calibration ion chamber (a.k.a. EGG counter) manufactured by Far West Technologies in conjunction with larger secondary ion chambers. The secondary ion chambers are used to measure integrated dose and cut the beam off when a specific dose has been reached. The dosimetry unit is rad(H_2O) and must be converted to rad(Si) and then scaled by the LET of the incident beam in order to calculate the particle fluence.

In order to take advantage of the generous beam spot, jigs were made to hold four separate, coplanar DUTs – three SRAMs and one SRAM-based FPGA. Irradiations that took place at normal incidence have the DUT's surface normal parallel with the beam vector, making the DUT's surface the xy-plane. The coordinate system for experiments at angle is described by the tilt and roll angles relative to the normal incidence setup. (90° tilt, 0° roll) requires a 90° rotation about the x- or y-axis. (90° tilt, 90° roll) first requires a 90° rotation about the z-axis, swiveling the DUT perpendicular to the beam, followed by a 90° rotation about the x- or y-axis. The latter two tilted conditions can be viewed as irradiating the DUT through one edge and then the other. In terms of spherical coordinates, tilt is a displacement in the polar angle ϕ and roll is a displacement in the azimuthal angle θ.

III. Experimental Results

A. Static Random Access Memories

Three SRAMs from two vendors, A and B, were exposed to the iron beam at the NSRL. Of the three, two are 65 nm and one is 45 nm. One of the 65 nm SRAMs and the 45 nm SRAM are a silicon-on-insulator (SOI) process from vendor A; the remaining 65 nm part is a bulk complementary metal oxide semiconductor (CMOS) part from vendor B. Vendor A's 65 nm SOI SRAM is 1 Mbit and their 45 nm SOI SRAM is 36 Mbit. Vendor B's bulk CMOS SRAM is 8 Mbit. We tested all three SRAMs under static conditions. The tester writes a specific data pattern to the DUT, the DUT is irradiated, and

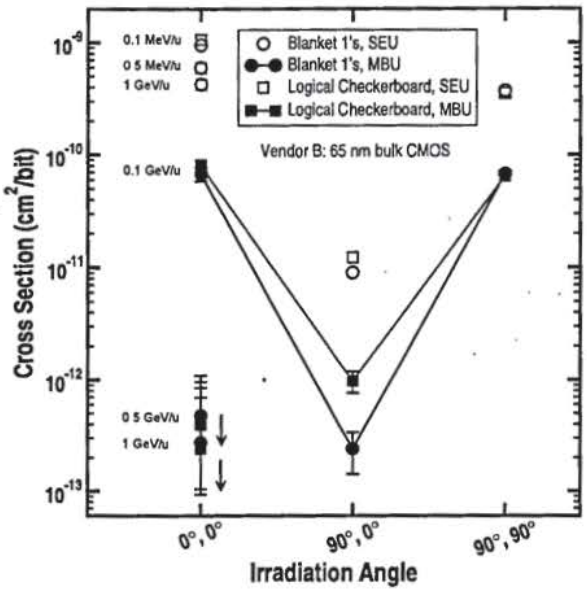

Fig. 5. Vendor B's 65 nm, 8 Mbit bulk CMOS SRAM ^{56}Fe data. The abscissa categories are given as (ϕ, θ) tilt/roll angle pairs. The legend shows the data pattern and the type of upset cross section. Irradiation energies are given at normal incidence since the data points are degenerate. The DUT was biased at $V_{DD} = 1.2$ V for all exposures. Limiting cross sections are indicated by downward-pointing arrows.

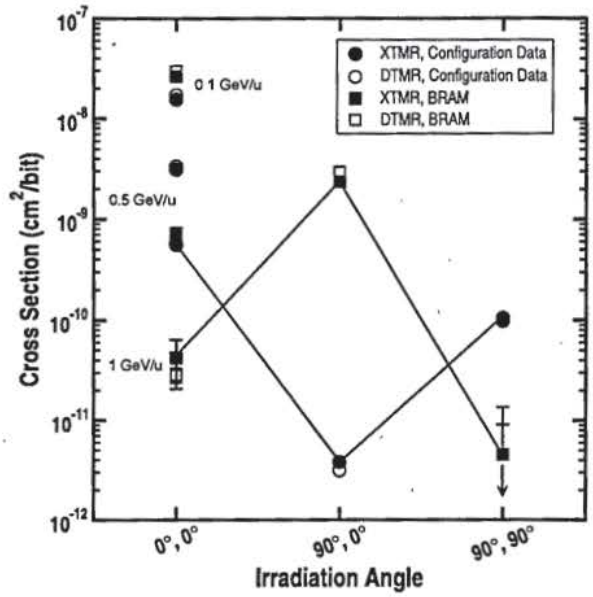

Fig. 6. Vendor C's 90 nm bulk CMOS FPGA ^{56}Fe static data. The abscissa categories are given as (ϕ, θ) tilt/roll angle pairs. The legend shows the data pattern and the type of upset cross section. Irradiation energies are given at normal incidence since the data points are degenerate. The single limiting cross section is indicated by a downward-pointing arrow.

then the contents of the memory are read back. This is different than either continuous read (errors can accumulate) or read-modify-write (continuous scrubbing) testing, both of which are dynamic methods.

$$\sigma_{\mathrm{SEU}} = \sum_{i=1}^{\infty} \frac{i \times \mathrm{Event}_{i_{\mathrm{bit}}}}{\Phi} \tag{2}$$

$$\sigma_{\mathrm{MBU}} = \sum_{i=2}^{\infty} \frac{\mathrm{Event}_{i_{\mathrm{bit}}}}{\Phi} \tag{3}$$

Vendor A's SEU and MBU cross sections for the 65 and 45 nm SOI SRAMs are shown in Fig. 4. The equations for the uncorrelated SEU and the correlated MBU cross sections are given by Eqs. 2 and 3 [12]. The SEU cross section is the total number of single-bit errors plus the multiplicity-corrected number of multi-bit errors divided by the uncorrected fluence. Since effective LET and effective fluence are either undefined or zero at a tilt angle of 90°, the standard right rectangular parallelepiped cosine corrections have been omitted. The MBU cross section is the number of MBU events involving two or more physically adjacent bits divided by the uncorrected fluence. Both the 65 and 45 nm SRAMs were irradiated at normal incidence, a tilt of 90° and roll of 0°, and at a tilt of 90° and a roll of 90°. All three of these irradiations were conducted with the 1 GeV/u ^{56}Fe beam.

Vendor A's MBU pattern and orientation dependence is a result of the SRAM cell construction and in turn the location of off-state transistors in proximity [16], [19]. The location of these off-state transistors can change depending on the data pattern, shown in Fig. 4(b), or stay the same, as shown in Fig. 4(a).

Vendor B's SEU and MBU cross sections are shown in Fig. 5. This 8 Mbit bulk CMOS SRAM was exposed at 0.1, 0.5, and 1 GeV/u at normal incidence and at 1 GeV/u for the other two orientations – (90° tilt, 0° roll) and (90° tilt, 90° roll). Two data patterns were written to the memory – FF for blanket 1's and AA for a logical checkerboard. There is no significant difference in response for these two patterns unlike Vendor A's SRAM. The data in Fig. 5 show a definite cross section dependence on grazing orientation with (90° tilt, 90° roll) being the most sensitive. At this orientation both the SEU and MBU cross sections are larger than at the orthogonal roll angle with the same tilt. This indicates that the physical layout is responsible for the elevation in upset cross section [12], [25]. Physically adjacent MBUs as large as ten bits were observed at this orientation, though this number is uncertain due to unavoidable false-positive MBUs.

B. Field Programmable Gate Array

A 90 nm bulk CMOS, SRAM-based FPGA from Vendor C was exposed to the same beams as Vendor A's SRAM – 0.1, 0.5, and 1 GeV/u ^{56}Fe at normal incidence and 1 GeV/u ^{56}Fe at (90° tilt, 0° roll) and (90° tilt, 90° roll). The results are shown in Fig. 6. A biased DUT was placed in the beam and the clocks were held static. The DUT underwent read back following exposure, recording the full contents of the configuration memory, which includes the logic configuration and block RAM (BRAM). The number of bits in error were calculated and then separated into configuration data and BRAM. This process was completed for two different, redundant FPGA designs – XTMR and DTMR [26]. The cross section for each of these designs' configuration data and BRAM were calculated separately and are reported in Fig. 6.

IV. Discussion

The SRAM results are consistent with the fundamental differences between bulk CMOS and SOI technologies. The bulk technology has a thicker sensitive volume with many devices residing in the same n- and p-wells, making a large number of bits simultaneously susceptible to upset. This feature, while increasing the probability of high-multiplicity MBUs, also removes data pattern sensitivity since charge transport within the wells means that it is unnecessary for the incident ion to physically strike the necessary nodes to cause a cell state change.

The SOI SRAM data have a definite pattern dependence in addition to the orientation sensitivity observed with the bulk CMOS SRAM. Since each SOI SRAM cell, and indeed some individual transistors within the SRAM cell, are isolated by oxide, the charge transport relevant in the bulk SRAM technology no longer applies. MBU in an SOI SRAM requires that the incident ion, or daughter particles in the case of indirect ionization, strike all the cells necessary to cause upset; charge transport only plays a small role.

The FPGA data, shown in Fig. 6, exhibit similar behavior to the SRAM data presented in Figs. 4 and 5, partly because the FPGA is SRAM-based, though the functionality of the two device types is very different. It is interesting to note that the configuration data and BRAM have opposing trends at (90° tilt, 0° roll) and (90° tilt, 90° roll), yielding information about the orientation of internal data storage.

We had to conduct static tests on all four of these devices, which presents challenges when reducing and interpreting the data, particularly when testing the devices at a tilt angle of 90°. In this orientation, only a small subset of the full SRAM or configuration memory is facing the beam, increasing the likelihood of false-positive MBUs, since multiple-bit upsets are filtered based on physical adjacency. A useful formula for calculating the probability of false-positive MBUs for a static test given the total number of upsets and total number of bits was presented by E. H. Cannon [16].

However, this formula assumes that each bit has an equally likely probability of being upset, a condition violated by conducting irradiations at a tilt angle of 90°. The LET of 1 GeV/u ^{56}Fe will not change as it passes through the target, so each bit should have an equal chance of being upset based on the phenomenology of a Weibull [27] or log normal [28] failure distribution, both of which rely on LET; this is not the source of error. The error comes from the solid angle occupied by the bits exposed to the beam and an alignment of bits parallel to the beam vector. The extreme case for this would be a DUT perpendicular to a perfectly collimated beam, neither of which are true for a realistic experiment. Regardless of the setup, storage device tests at extreme angles should scrub the memory dynamically whenever possible in order to avoid doubly-flipped bits and error pileup leading to an increase in the probability of physically-adjacent single-bit upsets that will in turn be interpreted as multiple-bit upsets.

While we focused this work on experimental results, these data provide a strong argument for the use of radiation transport simulations to extend standard heavy ion testing and evaluation to more realistic on-orbit environments. One of the most successful international collaborations on this front is the GEANT4 Space Users Group [29]. Simulations not only provide suitable space environments, they also yield far more granularity in their solutions. These details are useful for uncovering SEE mechanisms and making design decisions that impact system-level hardness assurance.

V. Conclusion

This is the first time the NSRL facility has been used to irradiate highly-scaled commercial CMOS and SOI technologies. The 1 GeV/u ^{56}Fe beam allowed true 90° grazing angle irradiation of SRAM and FPGA parts without special die or package preparation. These experiments represent the current state-of-the-art for accelerated ground testing and allow for upset characterization with a realistic GCR heavy ion beam.

While it would be ideal to be able to execute these kind of experiments on a regular basis, experimental logistics and cost are significant barriers. The good news is that for most parts this kind to testing is unnecessary. Standard laboratory tilt angles should reveal the limiting case trends shown in Figs. 4, 5, and 6. However, these data also underscore the fact that data pattern and roll angle can and do play a significant role in upset cross section and thus are relevant concerns for single-event hardness assurance and must be investigated.

Acknowledgment

The authors would like to thank A. Rusek, M. Seiverts, P. Guida and the rest of the staff at the NSRL and the BNL Collider-Accelerator Department for excellent management and their not insignificant assistance in completing a successful test campaign at a new facility.

References

[1] R. A. Reed, J. Kinnison, J. C. Pickel, S. Buchner, P. W. Marshall, S. Kniffin, and K. A. LaBel, "Single-event effects ground testing and on-orbit rate prediction methods: the past, present, and future," *IEEE Trans. Nucl. Sci.*, vol. 50, no. 3, pp. 622–634, Jun. 2003.

[2] M. A. Xapsos, "Modeling the space radiation environment," in *Nuclear and Space Radiation Effects Conf. Short Course*. Ponte Vedra Beach, FL: IEEE, 2006, pp. 1–62 Section II.

[3] R. A. Nymmik, M. I. Panasyuk, T. I. Pervaja, and A. A. Suslov, "A model of galactic cosmic ray fluxes," *Nucl. Tracks Radiat. Meas.*, vol. 20, no. 3, pp. 427–429, 1992.

[4] G. Badhwar and P. M. O'Neill, "Galactic cosmic radiation model and its applications," *Adv. Space. Res.*, vol. 17, no. 2, pp. 7–17, 1996.

[5] J. Feynman and S. B. Gabriel, "High-energy charged particles in space at one astronomical unit," *IEEE Trans. Nucl. Sci.*, vol. 43, no. 2, pp. 344–352, Apr. 1996.

[6] R. A. Nummik, M. I. Panasyuk, and A. A. Suslov, "Galactic cosmic ray flux simulation and prediction," *Adv. Space Res.*, vol. 17, no. 2, pp. 19–30, 1996.

[7] A. J. Tylka, J. H. Adams Jr, P. R. Boberg, B. Brownstein, W. F. Dietrich, E. O. Flueckiger, E. L. Petersen, M. A. Shea, D. F. Smart, and E. C. Smith, "CREME96: a revision of the Cosmic Ray Effects on Micro-Electronics Code," *IEEE Trans. Nucl. Sci.*, vol. 44, no. 6, pp. 2150–2160, Dec. 1997.

[8] [Online]. Available: https://www.jyu.fi/fysiikka/en/research/accelerator/radef/

[9] J. A. Pellish, R. A. Reed, A. K. Sutton, R. A. Weller, M. A. Carts, P. W. Marshall, C. J. Marshall, R. Krithivasan, J. D. Cressler, M. H. Mendenhall, R. D. Schrimpf, K. M. Warren, B. D. Sierawski, and G. F. Niu, "A generalized SiGe HBT single-event effects model for on-orbit event rate calculations," *IEEE Trans. Nucl. Sci.*, vol. 54, no. 6, pp. 2322–2329, Dec. 2007.

[10] R. A. Reed, M. A. Carts, P. W. Marshall, C. J. Marshall, O. Musseau, P. J. McNulty, D. R. Roth, S. Buchner, J. Melinger, and T. Corbiere, "Heavy ion and proton-induced single event multiple upset," *IEEE Trans. Nucl. Sci.*, vol. 44, no. 6, pp. 2224–2229, Dec. 1997.

[11] A. B. Campbell, O. Musseau, V. Ferlet-Cavrois, W. J. Stapor, and P. T. McDonald, "Analysis of single event effects at grazing angle [CMOS SRAMs]," *IEEE Trans. Nucl. Sci.*, vol. 45, no. 3, pp. 1603–1611, Jun. 1998.

[12] A. D. Tipton, J. A. Pellish, J. M. Hutson, R. Baumann, X. Deng, A. Marshall, M. A. Xapsos, H. S. Kim, M. R. Friendlich, M. J. Campola, C. M. Seidleck, K. A. LaBel, M. H. Mendenhall, R. A. Reed, R. D. Schrimpf, R. A. Weller, and J. D. Black, "Device-orientation effects on multiple-bit upset in 65 nm SRAMs," *IEEE Trans. Nucl. Sci.*, vol. 55, no. 6, pp. 2880–2885, Dec. 2008.

[13] C. W. Slayman, "Cache and memory error detection, correction, and reduction techniques for terrestrial servers and workstations," *IEEE Trans. Device Mater. Rel.*, vol. 5, no. 3, pp. 397–404, Sep. 2005.

[14] N. Seifert, P. Slankard, M. Kirsch, B. Narasimham, V. Zia, C. Brookreson, A. Vo, S. Mitra, B. Gill, and J. Maiz, "Radiation-induced soft error rates of advanced cmos bulk devices," in *Int. Reliability Physics Symp.*, Mar. 2006, pp. 217–225.

[15] H. Quinn, K. Morgan, P. Graham, J. Krone, M. Caffrey, and K. Lundgreen, "Domain crossing errors: Limitations on single device triple-modular redundancy circuits in Xilinx FPGAs," *IEEE Trans. Nucl. Sci.*, vol. 54, no. 6, pp. 2037–2043, Dec. 2007.

[16] E. H. Cannon, M. S. Gordon, D. F. Heidel, A. J. KleinOsowski, P. Oldiges, K. P. Rodbell, and H. Tang, "Multi-bit upsets in 65 nm SOI SRAMs," in *Int. Reliability Physics Symp.*, May 2008, pp. 195–201.

[17] N. Seifert, B. Gill, K. Foley, and P. Relangi, "Multi-cell upset probabilities of 45 nm high-k + metal gate SRAM devices in terrestrial and space environments," in *Int. Reliability Physics Symp.*, May 2008, pp. 181–186.

[18] H. Quinn, P. Graham, and B. Pratt, "An automated approach to estimating hardness assurance issues in triple-modular redundancy circuits in Xilinx FPGAs," *IEEE Trans. Nucl. Sci.*, vol. 55, no. 6, pp. 3070–3076, Dec. 2008.

[19] D. F. Heidel, P. W. Marshall, J. A. Pellish, K. P. Rodbell, K. A. LaBel, J. R. Schwank, S. E. Rauch, M. Hakey, M. D. Berg, C. Castaneda, P. E. Dodd, M. R. Friendlich, A. M. Phan, C. M. Seidleck, M. R. Shaneyfelt, and M. A. Xapsos, "Single-event upsets and multiple-bit upsets on a 45 nm SOI SRAM," *IEEE Trans. Nucl. Sci.*, vol. 56, no. 6, in press, 2009.

[20] K. P. Rodbell, D. F. Heidel, H. H. K. Tang, M. S. Gordon, P. Oldiges, and C. E. Murray, "Low-energy proton-induced single-event-upsets in 65 nm node, silicon-on-insulator, latches and memory cells," *IEEE Trans. Nucl. Sci.*, vol. 54, no. 6, pp. 2474–2479, Dec. 2007.

[21] D. F. Heidel, P. W. Marshall, K. A. LaBel, J. R. Schwank, K. P. Rodbell, M. C. Hakey, M. D. Berg, P. E. Dodd, M. R. Friendlich, A. D. Phan, C. M. Seidleck, M. R. Shaneyfelt, and M. A. Xapsos, "Low energy proton single-event-upset test results on 65 nm SOI SRAM," *IEEE Trans. Nucl. Sci.*, vol. 55, no. 6, pp. 3394–3400, Dec. 2008.

[22] B. D. Siearwski, J. A. Pellish, R. A. Reed, R. D. Schrimpf, R. A. Weller, M. H. Mendenhall, J. D. Black, M. A. Xapsos, R. C. Baumann, X. Deng, and A. D. Tipton, "Impact of low-energy proton induced upsets on test methods and rate predictions," *IEEE Trans. Nucl. Sci.*, vol. 56, no. 6, in press, 2009.

[23] Private communication with Dr. Michael Siverts, Brookhaven National Laboratory. [Online]. Available: http://www.bnl.gov/medical/NASA/NSRL_description.asp

[24] Y. M. Charara, L. W. Townsend, T. A. Gabriel, C. J. Zeitlin, L. H. Heilbronn, and J. Miller, "HETC-HEDS code validation using laboratory beam energy loss spectra data," *IEEE Trans. Nucl. Sci.*, vol. 55, no. 6, pp. 3164–3168, Dec. 2008.

[25] J. M. Hutson, J. A. Pellish, A. D. Tipton, G. Boselli, M. A. Xapsos, H. Kim, M. Friendlich, M. Campola, S. Seidleck, K. LaBel, A. Marshall, X. Deng, R. Baumann, R. A. Reed, R. D. Schrimpf, R. A. Weller, and L. W. Massengill, "Evidence for lateral angle effect on single-event latchup in 65 nm srams," *IEEE Trans. Nucl. Sci.*, vol. 56, no. 1, pp. 208–213, Feb. 2009.

[26] M. D. Berg, "Example 1: Trading ASIC and FPGA considerations for system insertion," in *Nuclear and Space Radiation Effects Conf. Short Course*. Quebec City, Quebec CN: IEEE, 2009, pp. 1–72 Section V.

[27] J. C. Pickel, "Single-event effects rate prediction," *IEEE Trans. Nucl. Sci.*, vol. 43, no. 2, pp. 483–495, Apr. 1996.

[28] E. L. Petersen, "Cross section measurements and upset rate calculations," *IEEE Trans. Nucl. Sci.*, vol. 43, no. 6, pp. 2805–2813, Dec. 1996.

[29] GEANT4 Space Users Group. [Online]. Available: http://geant4.esa.int/